Journal of Power Sources 248 (2014) 951–961

Contents lists available at ScienceDirect

Journal of Power Sources

journal homepage: www.elsevier.com/locate/jpowsour

Enhancing water retention and low-humidity proton conductivity of sulfonated poly(ether ether ketone) composite membrane enabled by the polymer-microcapsules with controllable hydrophilicity–hydrophobicity

Guangwei He [a], Yifan Li [a], Zongyu Li [a], Lingli Nie [a], Hong Wu [a], Xinlin Yang [b], Yuning Zhao [a], Zhongyi Jiang [a,*]

[a] Key Laboratory for Green Chemical Technology of Ministry of Education, School of Chemical Engineering and Technology, Tianjin University, Tianjin 300072 China

[b] Key Laboratory of Functional Polymer Materials, Ministry of Education, Institute of Polymer Chemistry, Nankai University, Tianjin 300071, China

HIGHLIGHTS

- Polymeric microcapsules with tunable hydrophilicity–hydrophobicity were prepared.
- The four kinds of microcapsules possessed different water retention.
- SPEEK/microcapsules composite membranes were prepared.
- The composite membranes exhibited enhanced low-humidity proton conductivity.

ARTICLE INFO

Article history:
Received 20 June 2013
Received in revised form
27 September 2013
Accepted 6 October 2013
Available online 15 October 2013

Keywords:
Polymer microcapsules
Controllable hydrophilicity–hydrophobicity
Sulfonated poly(ether ether ketone) membranes
Water retention
Proton conductivity

ABSTRACT

Four kinds of polymer microcapsules (PMCs) with different hydrophilicity–hydrophobicity are synthesized via distillation–precipitation polymerization (polymer microcapsules form by self-crosslinking of monomers/crosslinkers in this process) and incorporated into sulfonated poly(ether ether ketone) (SPEEK) matrix to prepare composite membranes. To improve the water retention of the PMCs, the hydrophilicity–hydrophobicity of the PMCs is manipulated by regulating the proportion of hydrophilic ethylene glycol dimethacrylate (EGDMA) and hydrophobic divinylbenzene (DVB) crosslinkers in the synthesis formula. The hydrophilicity of the PMCs decreases with increasing the content of polyDVB in the PMCs. The four kinds of PMCs exhibit different water retention properties. The PMCs with appropriate hydrophilic/hydrophobic balance (EGDMA: DVB = 1:1) possess the best water retention properties. Incorporation of PMCs into SPEEK matrix enhances the water-retention properties, and consequently increases proton conductivity to 0.0132 S cm^{-1} under 20% relative humidity, about thirteen times higher than that of the SPEEK control membrane. Moreover, the incorporation of PMCs reduces the activation energy for proton conduction and the methanol permeability of the membranes. This study may be helpful to rational design of excellent water-retention materials.

1. Introduction

Nanoengineered multifunctional polymer microcapsules (PMCs) with tailored structures and properties have stimulated great interest due to their wide applications, spanning medicine, biotechnology, catalysis and synthetic chemistry [1–3]. Recently, PMCs have been demonstrated as effective water-retention and proton-conduction fillers for proton exchange membranes (PEMs) under operation conditions (high temperature and/or low humidity) [4–6], which is greatly desired for high fuel cell performances [7–10]. The PMCs, mimicking the water-storage mechanisms in plant cells, possess high water uptake and slow water release [5]. The dehydration of the resulting membrane was remarkably retarded by the incorporation of these versatile fillers with tailored structures and tunable chemical compositions, resulting in notably enhanced proton conductivity under operation conditions. Moreover, the high density of proton conductive groups in the shell of the PMCs can further promote proton conduction [5,6,11].

* Corresponding author. Tel./fax: +86 22 23500086.
E-mail address: zhyjiang@tju.edu.cn (Z. Jiang).

0378-7753/$ – see front matter © 2013 Elsevier B.V. All rights reserved.
http://dx.doi.org/10.1016/j.jpowsour.2013.10.017

A series of PMCs, bearing different functional groups such as carboxylic acid [5], sulfonic acid [4,5], phosphoric acid [12,13] and imidazole [6] were designed and incorporated into PEMs to enhance their water retention and proton conductivity. For instance, the chitosan composite membranes based on carboxylic acid functionalized PMCs exhibited a proton conductivity one to two orders of magnitude higher than that of chitosan control membrane under 20% relative humidity (RH) [5]. Incorporation of sulfonated polystyrene microcapsules into Nafion sustained proton conductivity up to 0.01 S cm^{-1} at 120 °C, while the proton conductivity of the control Nafion membrane was below 0.0013 S cm^{-1} [4]. The Single H_2-PEMFC test at 70 °C using dry H_2/O_2 verified the impactful role of PMCs functionalized with sulfonic acid or carboxylic acid in sustaining higher proton flux as compared to Nafion control membrane [14]. All these results indicate the potential of PMCs for fuel cell applications. Moreover, the variability of physical structures and chemical compositions endow the PMC with a large scope of improvement in terms of water retention and proton conduction. Although various studies have well-established the influence of functional groups, lumen sizes, and shell thicknesses of the PMCs on their water retention and proton conduction properties, one issue unexplored in PMCs is the role of hydrophilicity–hydrophobicity of PMCs in water retention and proton conduction properties of the PMCs.

It is widely accepted that hydrophilic substance in polymer matrix binds water through hydrogen bond or electrostatic interaction and facilitates water sorption and diffusion, while hydrophobic substance in polymer matrix has a weak interaction with water and suppresses water sorption and diffusion [15]. Thus, manipulating the hydrophilicity–hydrophobicity of PMCs can control water sorption and water release rate. In nature, a common strategy for desert plant to restrain water from releasing is evolving a layer of cuticle (hydrophobic fatty acid) with the ability of decreasing moisture evaporation rate [16–18]. Moreover, the currently employed approaches to improve water retention of PEMs focused on improving hydrophilicity of membrane [5,19], while enhancing water retention by adjusting hydrophilicity–hydrophobicity of membrane has been rarely involved. Therefore, it is essential that improved water retention of PEMs (enhanced water uptake and decreased water release) can be obtained by rationally tuning the hydrophilicity–hydrophobicity of PMCs.

In this study, both the water retention and low-humidity proton conductivity of SPEEK composite membrane were enhanced by the incorporation of polymer microcapsules with tunable hydrophilicity–hydrophobicity, which was controlled by regulating the proportion of hydrophilic ethylene glycol dimethacrylate (EGDMA) and hydrophobic divinylbenzene (DVB) crosslinkers in the distillation–precipitation polymerizations (polymer microcapsules formed by self-crosslinking of monomers/crosslinkers in this process) [20]. SPEEK is chosen as the matrix polymer on account of its outstanding thermomechanical stability, low cost and low fuel crossover features [8,21,22]. Moreover, the physiochemical and methanol barrier properties of the membranes were investigated.

2. Experimental

2.1. Materials and chemicals

Ethylene glycol dimethacrylate (EGDMA), divinylbenzene (DVB, 80% divinylbenzene isomers) and tetraethyl orthosilicate (TEOS) were supplied by Alfa Aesar and used without further purification. 3-(Methacryloxy) propyltrimethoxysilane (MPS) were supplied by Aldrich and distilled under vacuum. Methacrylic acid (MAA) was purchased from Tianjin Guangfu Fine Chemical Engineering Institute and purified by vacuum distillation. 2,2′-Azoisobutyronitrile (AIBN) was provided by Tianjin Guangfu Fine Chemical Engineering Institute and recrystallized from methanol. Acetonitrile was supplied by Tianjin Kewei Ltd. and was dried over calcium hydride and purified by distillation. Poly(ether ether ketone) (Victrex®PEEK, grade 381G) was supplied by Nanjing Yuanbang Engineering Plastics Co., Ltd. Dimethylformamide (DMF), sulfuric acid and methanol were supplied from Tianjin Kewei Ltd. De-ionized water was used throughout the experiment.

2.2. Synthesis of the PMCs and SPEEK

The synthesis of polymer microcapsules was illustrated in Fig. 1. Silica microspheres with diameter around 200 nm were synthesized according to Stöber method [23]: TEOS was added into the mixture of ethanol, water and aqueous solution of ammonium hydroxide under vigorous stirring at 30 °C for 24 h. Excess MPS was then added into the silica mixture with a reaction time of 24 h to modify the silica with carbon–carbon double bonds. The coating of polymer on MPS-modified silica spheres was carried out by distillation–precipitation polymerization in acetonitrile [5,20]. In a dried 100 ml flask attached to a fractionating column, Liebig condenser, and receiver, 0.20 g of silica particles was dispersed into 80 ml acetonitrile assisted by sonication. The monomer MAA (0.35 ml, 0.371 g), crosslinker EGDMA (0.65 ml, 0.624 g), and initiator AIBN (0.02 g, 2 wt% relative to the comonomers) were then dissolved into the MPS-modified silica solution. The mixture was heated from ambient temperature till boiling state and then the solvent was distilled from the reaction system. After 40 ml of acetonitrile was distilled out, the reaction was terminated and the resultant hybrid microspheres were purified by three cycles of ultracentrifugation, decanting, and resuspension in acetonitrile. Two-stage polymerization was utilized to get the polymer shell with controlled thickness and uniform shape. Three parallel syntheses were carried out using MAA as monomer and different crosslinkers, including EGDMA–DVB mixed crosslinker with a volume ratio of 3:1 and 1:1, and neat DVB crosslinker. The volume ratio of the crosslinker fraction in the comonomer feed was maintained as 0.65. The synthesized hybrid microspheres were etched by HF solution (10 wt%) for 2 h followed by several centrifugation/washing cycles in water till neutral pH was reached. The four types of PMCs with a constant MAA ratio as 35 vol% were prepared via altering the crosslinker: neat EGDMA, EGDMA–DVB with a volume ratio of 3:1 and 1:1, and neat DVB, which were designated as PMC-I, PMC-II, PMC-III and PMC-IV, respectively.

SPEEK was synthesized by sulfonation of PEEK: PEEK was dried for 24 h in a vacuum oven at 60 °C. The dried PEEK (28.0 g) was then dissolved into concentrated sulfuric acid (95–98 wt%, 200 ml) at room temperature. The reaction mixture was stirred vigorously at 50 °C for 9.5 h, cooled to room temperature, and then added into excessive cold water under continuous agitation. The precipitated SPEEK was washed with water till pH of 7.0 and then dried, first at room temperature for 48 h and then at 60 °C for 24 h under vacuum. The degree of sulfonation of SPEEK was 68.2% determined by titration method.

2.3. Preparation of the membranes

A certain amount of the PMCs were dispersed into DMF (3.0 ml) solution under ultrasonic treatment for 12 h. Simultaneously, SPEEK (0.65 g) was dissolved into DMF (4.0 ml) solution and stirred vigorously for 24 h at room temperature. The two solutions were then mixed under vigorous stirring for 2 h followed by 1 h ultrasonic treatment. The mixture was cast onto a glass plate and dried at 60 °C in an oven for 12 h followed by drying at 80 °C for another 12 h. The membrane was removed from the glass plate by

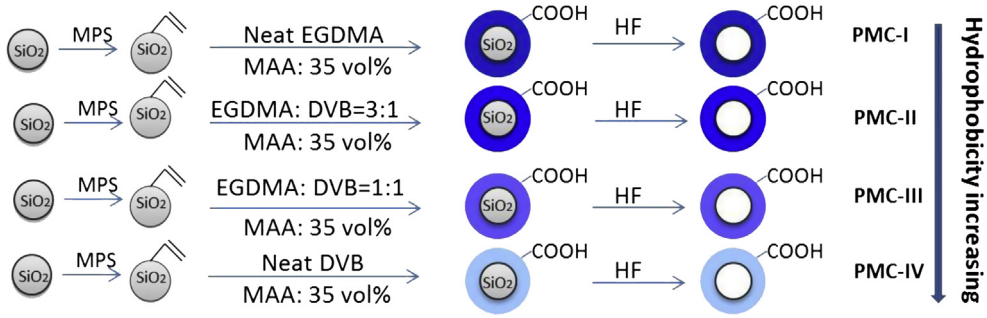

Fig. 1. Schematic illustration for synthesis of polymer microcapsules.

immersing the glass plate in water. The composite membranes were designated as SPEEK/PMC-N-*X*, where N (=I, II, III, or IV) represented the type of the synthesized PMC, and *X* (=2.5, 5, 10 or 15) referred to the weight percentage of the filler relative to the SPEEK matrix. The SPEEK control membrane was fabricated according to the above procedure and designated as SPEEK. The average thickness of the resultant membranes was within the range of 60–80 μm.

2.4. Characterizations

The morphology of the PMCs was characterized by Transmission electron microscopy (TEM, Tecnai G2 20 S-TWIN). Field emission scanning electron microscope (FESEM, Nanosem 430) was utilized to observe the cross-sectional morphology of the membranes after the membranes being freeze-fractured in liquid nitrogen and then sputtered with a thin layer of gold. Fourier transform infrared spectra (FTIR) of the samples over the range of 4000–500 cm^{-1} were probed on a BRUKER Vertex 70 FTIR spectrometer equipped with a horizontal attenuated transmission accessory for powders and a horizontal attenuated total reflectance accessory for membranes. Zeta potential was detected using a Zeta PALS (Brookhaven Instrument Cooperation) through measuring the electrophoretic mobility of the PMCs at neutral pH and room temperature. Thermogravimetric analysis (TGA) was performed by a thermogravimetric analyzer (NETZSCH-TG209 F3) over a temperature range of 40–800 °C at a heating rate of 10 °C min^{-1} under a nitrogen atmosphere. The glass transition temperature (T_g) was determined by differential scanning calorimetry (DSC, 204 F1 NETZSCH) with a heating or cooling rate of 10 °C min^{-1} under nitrogen flow. The sample was preheated from 20 °C to 130 °C and then cooled to 90 °C and reheated to 260 °C.

2.5. Water uptake, water release, water retention, water state and area swelling measurements

Before measurements, the samples were dried in a vacuum oven at 80 °C and tested for weight and area (W_{dry}, A_{dry}). Subsequently, the samples were immersed in deionized water at room temperature till complete hydration and the weight (W_{wet}) and area (A_{wet}) of the membranes were obtained. The measurements were repeated three times, and the error was within ±5%. The water uptake and swelling were calculated by the equations given below:

$$\text{Water uptake}(\%) = \frac{W_{wet} - W_{dry}}{W_{dry}} \times 100 \quad (1)$$

$$\text{Area swelling}(\%) = \frac{A_{wet} - A_{dry}}{A_{dry}} \times 100 \quad (2)$$

Then the samples were set in a climate box with a constant temperature and humidity (40 °C and 20% RH) and weighed ($W_{wet\ t}$) at time *t*. Water release and water retention were calculated by Eqs. (3) and (4), respectively:

$$\text{Water release}(\%) = \frac{W_{wet} - W_{wet\ t}}{W_{wet} - W_{dry}} \times 100 \quad (3)$$

$$\text{Water retention}(\%) = \frac{W_{wet\ t} - W_{dry}}{W_{dry}} \times 100 \quad (4)$$

Water state of a hydrated sample was determined by the DSC with a temperature scan speed of 5 °C min^{-1} ranging from −50 to 50 °C. The free water content was obtained by comparing the melting enthalpy of free water near 0 °C to the fusion heat of pure water (334 J g^{-1}). The bound water content is defined as total water minus the free water content in the sample.

2.6. Methanol permeability

Methanol permeability of the membranes was measured using a glass diffusion cell consisting of two identical volume compartments. The membrane was fully hydrated in water and then clamped tightly between the two compartments, one of which was filled with water and the other was filled with 2.0 M methanol solution. The concentration of methanol that permeated into the water compartment was determined by a gas chromatography (Agilent 6820) equipped with a Thermal Conductivity Detector (TCD) and a DB624 column. Methanol permeability (P, $cm^2\ s^{-1}$) was calculated according to Eq. (5):

$$P = \frac{SV_B l}{AC_{A0}} \quad (5)$$

where S is the slope of the straight line of concentration versus time, V_B is the solution volume of the receipt compartment, l, A, and C_{A0} are the membrane thickness, membrane area and methanol feed concentration, respectively.

2.7. Proton conductivity

Proton conductivity of the membranes at 25 °C, 100% RH and 40 °C, 20% RH was measured by the AC impedance spectroscopy method in vertical direction, and the membrane resistance was tested using a frequency response analyzer (FRA, Compactstat, IVIUM Tech.) with a potential of 20 mV in a frequency range of 10^6–1 Hz. The testing temperature and relative humidity was controlled by a climate box. The measurement was conducted at low temperatures to better analyze the function of water on proton transfer

in the PEMs. Temperature-dependent proton conductivity of the membranes in in-plane direction was tested with a two-point-probe conductivity cell [24] using an electrochemical workstation (PARSTAT 2273, Princeton). All samples were completely hydrated in water prior to measurement. Proton conductivity (σ, S cm^{-1}) was calculated using the Eq. (6):

$$\sigma = \frac{l}{AR} \tag{6}$$

where l is the membrane thickness, A the effective membrane area, and R the membrane resistance.

3. Results and discussion

3.1. Characterization of the polymer microcapsules

The four types of conductive PMCs were synthesized by the distillation–precipitation polymerization of MAA functional monomer (35 vol%) with different crosslinkers: neat EGDMA, EGDMA–DVB with a volume ratio of 3:1 and 1:1, and neat DVB to control their hydrophilicity–hydrophobicity. The morphology of the PMCs detected by TEM was shown in Fig. 2. Well-defined capsular configuration, dense shells, and large lumens were clearly presented for all the PMCs. Although identical silica cores (approximate 200 nm) were employed for the PMC synthesis, the lumen sizes (Table 1) of PMC-I and PMC-II were decreased to approximate 140 and 182 nm, respectively, due to the flexibility of polyEGDMA (PEGDMA) segments. The lumen sizes of PMC-III and PMC-IV maintained about 200 nm consistent with the silica core size because of the rigidity of polyDVB (PDVB) segments. The shell thickness (Table 1) of PMC-I, PMN-II, PMC-III and PMC-IV was around 94, 82, 81 and 77 nm, respectively, and the shell was robust enough to ensure the hollow structure. The functional groups in the shell were confirmed by the FTIR (Fig.3a). The FTIR absorption spectra of all PMCs presented the stretching vibration of carboxyl groups (peaks at 1720 and 1160 cm^{-1} attributable to the stretching vibration of C=O and COO–H groups from the polyMAA segments) [25,26]. The peaks at 706 cm^{-1} (assigning to the typical adsorption of phenyl group) in the FTIR spectra of the PMCs become stronger and stronger [27], which were consistent with the increase of DVB crosslinker for the design and synthesis of these microcapsules. The zeta-potential values of PMC-I, PMC-II, PMC-III and PMC-IV were around −34.12, −39.76, −44.22, and −37.96 mV, respectively, which may be originated from the almost near loading capacity of the carboxylic acid group. The TGA data (Fig. 3b) revealed that the

Table 1
The lumen size, shell thickness, zeta potential, water uptake, and water state of the polymer microcapsules.

Sample	Lumen size (nm)	Shell thickness (nm)	Zeta potential (mV)	Water uptake (%)	Free water (%)	Bound water (%)
PMC-I	141 ± 5	94 ± 5	−34.12	158.96	102.73	56.23
PMC-II	182 ± 3	82 ± 4	−39.76	166.71	112.03	54.67
PMC-III	200 ± 3	81 ± 4	−42.22	183.69	129.27	54.41
PMC-IV	200 ± 3	77 ± 3	−37.96	140.02	102.41	37.62

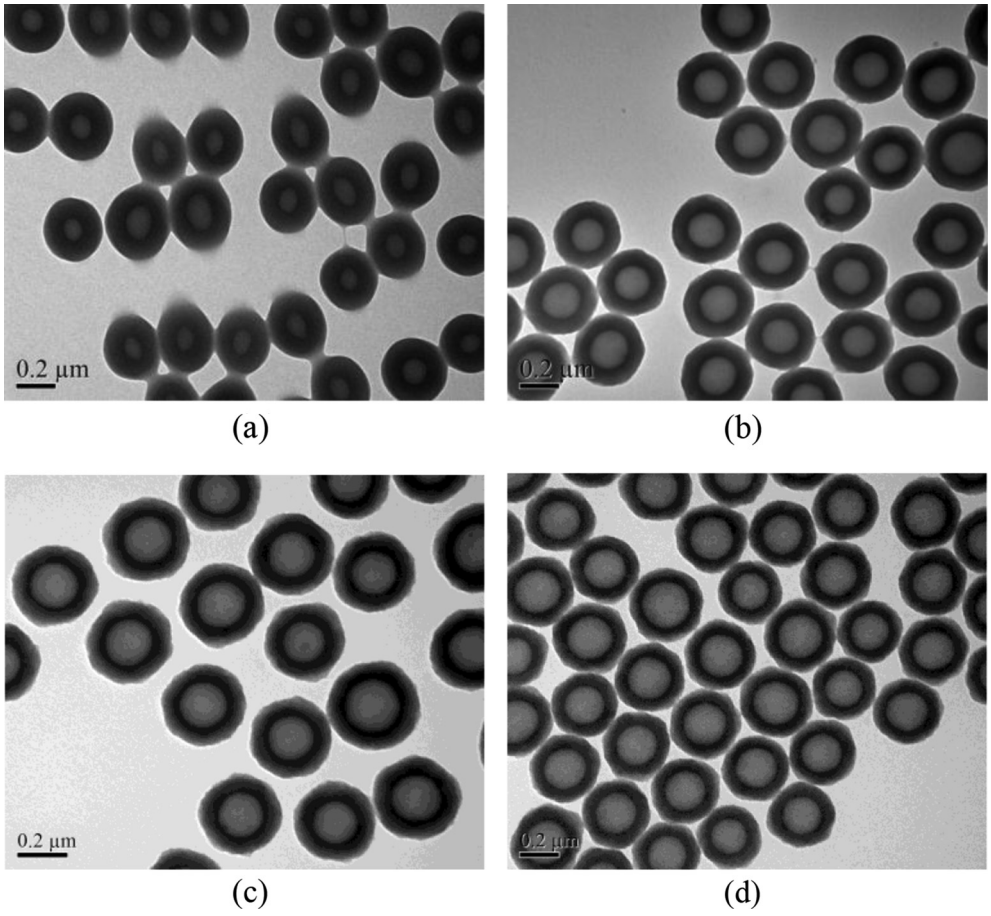

Fig. 2. TEM images of polymer microcapsules: (a) PMC-I, (b) PMC-II, (c) PMC-III, and (d) PMC-IV.

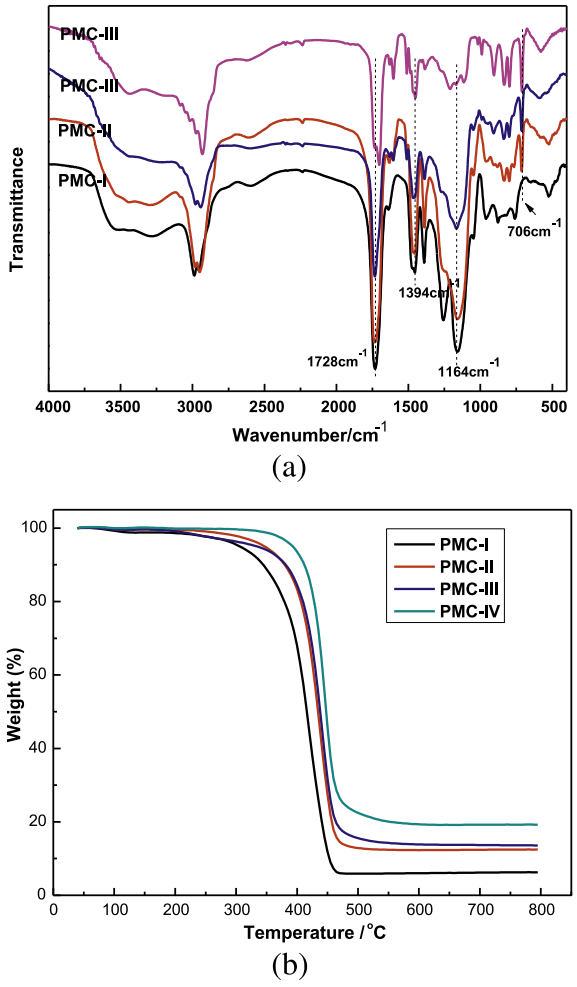

Fig. 3. (a) FTIR spectra of the polymer microcapsules, (b) TGA of the polymer microcapsules.

residual mass increased with increasing the PDVB content in the PMC, resulting from the higher thermal stability of PDVB components than that of PEGDMA components [26,28]. All these results confirmed that PMCs with defined structure and chemical composition were successfully synthesized. Since PEGDMA containing ethylene glycol unit was more hydrophilic than PDVB containing phenyl group [29,30], a reasonable deduction was that the hydrophilicity–hydrophobicity of PMCs can be controlled by regulating the PEGDMA/PDVB proportion. In other words, more PDVB content could render the PMC more hydrophobic, which was confirmed by the floating behavior upon water of the PMC-IV. It can be rationally conjectured from the above analysis that the hydrophilicity decreased in the order of PMC-I > PMC-II > PMC-III > PMC-IV with increasing PDVB segment content.

3.2. Characterization of the membranes

The PMCs were embedded into the SPEEK matrix to prepare composite membranes via solution casting method. FESEM images in Fig. 4 depicted that the SPEEK bulk was dense and void-free, and the PMCs maintained the pristine structure and distributed evenly within the SPEEK matrix. Fig. 4b–d displayed partial split of the microcapsules caused by the liquid nitrogen freeze-fracture. This behavior suggested good compatibility between the SPEEK matrix and the polymer fillers. FTIR spectra (Fig. 5a) of the SPEEK membranes showed that the characteristic peaks at 1219, 1077, and 1024 cm^{-1}, corresponding to the stretching vibration of O=S=O in $-SO_3H$ groups, were found in all the membranes [31,32]. The characteristic peaks of –COOH in the filled PMCs were overlapped by the peaks from SPEEK.

The contact angle (toward water) of the composite membranes and SPEEK control membrane was measured, as shown in Table 2. The results revealed that hydrophobicity of the membranes increased in the order: SPEEK/PMC-I-10 (75.3°) < SPEEK/PMC-II-10 (77.0°) < SPEEK (80.4°) < SPEEK/PMC-III-10 (80.6°) < SPEEK/PMC-IV-10 (90.8°), which were consistent with the hydrophilicity–hydrophobicity of the corresponding PMCs.

The glass transition temperatures of the pristine and composite membranes determined by DSC were given in Table 2. The SPEEK control membrane displayed a T_g of 213.1 °C, which was consistent with that reported in literature [33,34]. The composite membranes incorporated with PMC-I, PMC-II, PMC-III, and PMC-VI (10 wt% loading) possessed the T_g of 196.8, 206.3, 207.7, and 198.7 °C, respectively. The decrease of T_g may be attributed to the electrostatic repulsion between the –COOH groups on the surface of PMCs and $-SO_3H$ groups in the SPEEK matrix, which promoted the mobility of SPEEK chains.

TGA was used to determine the thermal stability of the composite membranes as shown in Fig. 5b. All membranes displayed a three-stage weight loss, i.e., the dehydration in the first weight loss region (40–150 °C), the desulfonation in the second weight loss region (240–372 °C) and the decomposition of main chains in the third weight loss region (400–800 °C) [32]. The char yield at 800 °C of composite membranes was lower than that of control membrane probably due to the presence of the PMCs which had a lower char yield compared with the SPEEK. Obviously, all the membranes were thermally stable up to 240 °C, adequate for practical application in PEMFC.

3.3. Water retention properties of the PMCs and the membranes

3.3.1. Water uptake

In the PEMs, adequate water uptake is essential to ensuring efficient vehicle-type and Grotthuss-type proton transfer [35,36]. Water uptake of the PMCs in Table 1 revealed that all the PMCs displayed excellent water storage capability with water uptakes above 140%, when compared with solid inorganic or organic particles (e.g., 26% for silica and 58% for polymer carboxylic acid spheres) [26,37]. The water uptake decreased in the order of PMC-III (183.7%) > PMC-II (166.7%) > PMN-I (159.0%) > PMN-IV (140%). The water state analyzed by DSC (Table 1) showed that the bound water content decreased with increasing the PDVB segments in PMC: PMC-I (56.2%) > PMC-II (54.7%) > PMN-III (54.4%) > PMN-IV (37.6%), which may be the result of higher affinity toward water of PEGDMA than that of PDVB segments. The larger lumen rendered PMC-III more space to store water, in turn possessing higher water uptake than that of PMC-I and PMC-II. A plausible explanation for low water uptake of PMC-IV was that its floating phenomenon upon water resultant from strong hydrophobicity caused the difficulty in obtaining a lumen full of water. Table 2 showed the water uptake and area swelling of the membranes. Embedment of PMCs increased water uptake from 40.6% for SPEEK control membrane to 42.3–57.2% for the composite membranes. The enhancement of water uptake of the membranes showed a positive correlation with the water storage capacity of the PMCs, indicating that the PMCs served as water reservoirs to provide additional space for water and hence to endow PMC-filled membranes with increased water uptake. For instance, the water uptake of the membranes based on PMC-III increased from 44.7 to 57.2% with the PMC-III content increasing from 2.5 to 15 wt%. Area swelling data showed that incorporation of PMCs enhanced area swelling from 28.3% for the

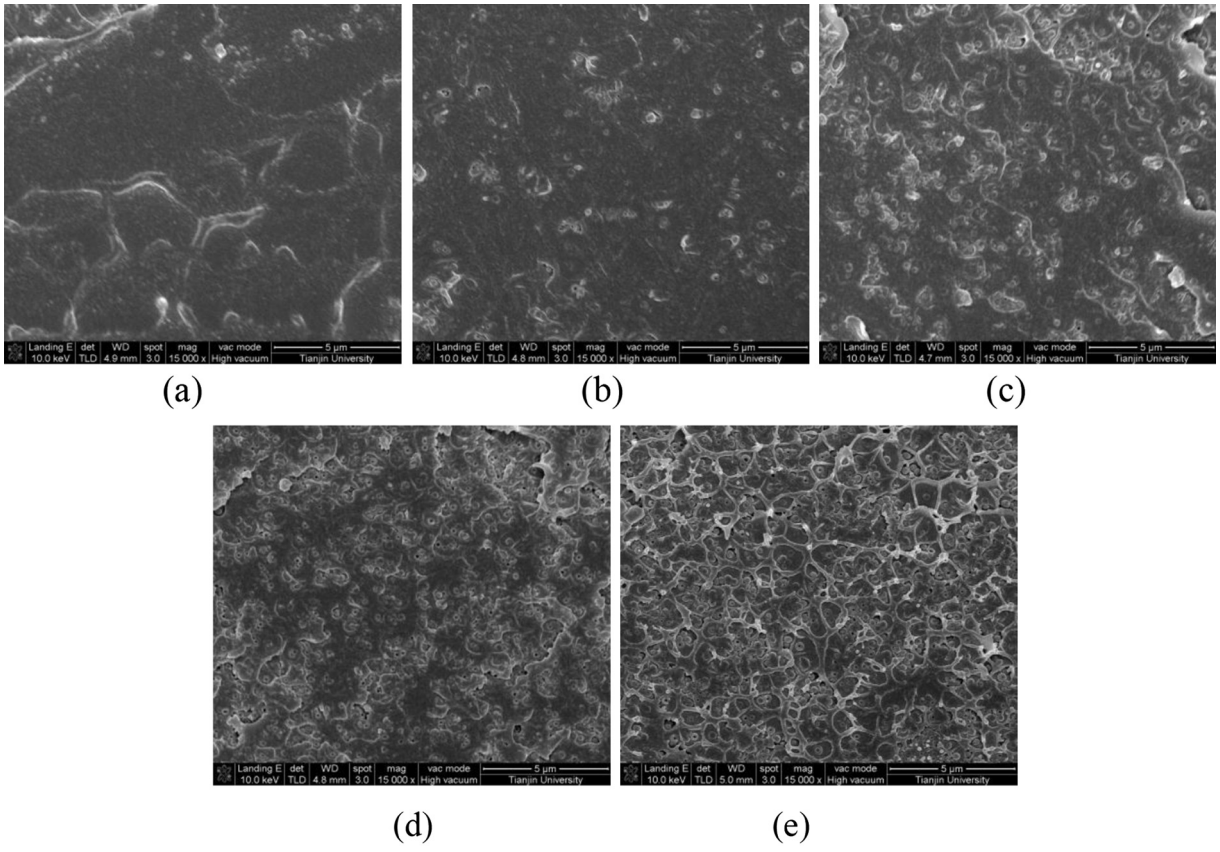

Fig. 4. FESEM images of the cross-sections of (a) SPEEK, (b) SPEEK/PMC-I-10, (c) SPEEK/PMC-II-10, (d) SPEEK/PASCs-III-10, and (e) SPEEK/PMC-IV membranes.

SPEEK control membrane to 30.7% for the 15 wt% PMC-III filled membrane. It can be deduced that the electrostatic repulsion between the PMCs and the SPEEK matrix played partial role in enhancing area swelling. Such an inappreciable increment of area swelling of the PMC-filled membranes was believed to be the result of the high-crosslinking and swelling-resistant features of the PMCs. Thus, this water-retention approach may provide a possibility of breaking the trade-off correlations between water uptake and swelling resistance of PEMs.

3.3.2. Water release

Besides water uptake, the dynamic water release is also crucial to guide the design of high-conduction PEM under low humidity. To elucidate the effect of hydrophilicity−hydrophobicity of PMCs on water release, the dynamic water release of the PMCs and the membranes at 40 °C and 20% RH were measured, as shown in Fig. 6a and 7 . The water release slopes (Fig. 6a) revealed that the water release rate of the PMCs decreased in the order of PMC-IV (S = 0.08) > PMC-I (S = 0.053) > PMC-II (S = 0.04) > PMC-III

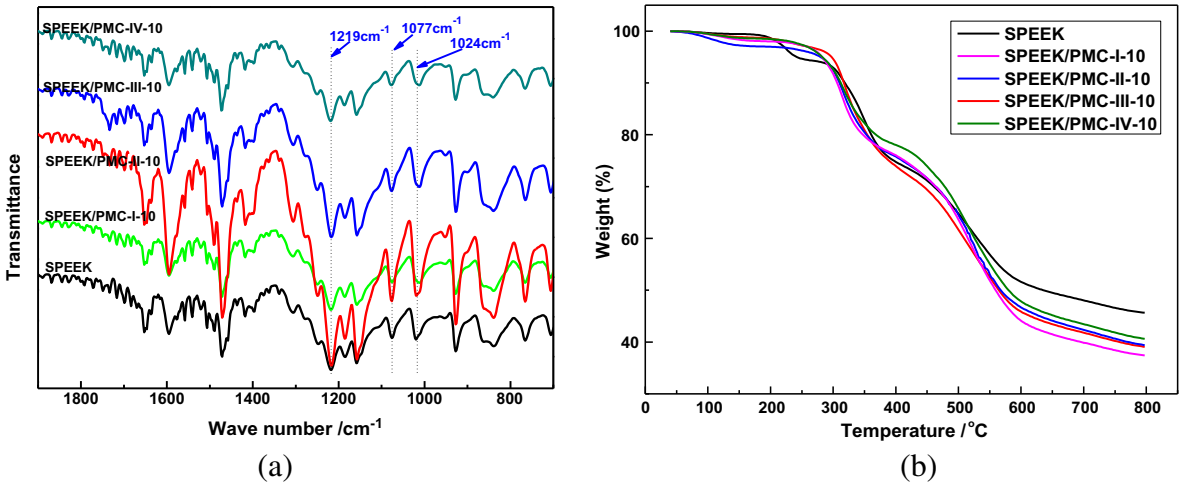

Fig. 5. (a) FTIR, and (b) TGA curves of the membranes.

Table 2
Water uptake, area swelling, methanol permeability, proton conductivity, contact angle, and glass-transition temperature of the membranes.

Membrane	Water uptake (%)[a]	Area swelling (%)	Methanol permeability (10^{-7} cm^2 s^{-1})	Proton conductivity (S cm^{-1})[a]	Contact angle (°)	T_g (°C)
SPEEK	40.64	28.26	9.10	0.0138	80.4	213.1
SPEEK/PMC-I-2.5	43.43	29.01	8.66	0.0150	–	–
SPEEK/PMC-I-5	47.22	30.85	8.23	0.0159	–	–
SPEEK/PMC-I-10	58.08	31.62	7.13	0.0163	75.3	196.8
SPEEK/PMC-I-15	53.70	32.82	6.68	0.0176	–	–
SPEEK/PMC-II-2.5	42.28	28.89	8.25	0.0151	–	–
SPEEK/PMC-II-5	48.62	30.40	7.87	0.0162	–	–
SPEEK/PMC-II-10	51.03	30.53	6.88	0.0177	77.0	206.3
SPEEK/PMC-II-15	54.28	31.02	6.57	0.0180	–	–
SPEEK/PMC-III-2.5	44.69	28.43	8.05	0.0152	–	–
SPEEK/PMC-III-5	49.21	29.20	7.47	0.0169	–	–
SPEEK/PMC-III-10	52.66	29.76	6.55	0.0176	80.6	207.7
SPEEK/PMC-III-15	57.21	30.73	6.46	0.0182	–	–
SPEEK/PMC-IV-2.5	42.61	28.18	7.65	0.0149	–	–
SPEEK/PMC-IV-5	45.95	28.62	7.18	0.0163	–	–
SPEEK/PMC-IV-10	47.26	29.39	6.59	0.0166	90.8	198.7
SPEEK/PMC-IV-15	51.22	30.04	6.29	0.0165	–	–

[a] Water uptake and proton conductivity at 25 °C.

($S = 0.032$). For PMC-I, PMC-II, and PMC-III, the water release rate decreased with the increase of their hydrophobicity. It was demonstrated that high bound water content and small lumen size of PMC was beneficial to retard water release, because the water in the lumen released outside through transforming from free water to bound water and then to free water, and the curvature-related effect lowered chemical potential of absorbed water [5]. However, the water release rate exhibited contrary results: the PMC-III with the lowest content of bound water and the largest lumen size showed the lowest water release. This tendency was presumably arisen from the increment of hydrophobic substance ratio, which obstructed water from releasing out of PMCs. Moreover, the PMC-III displayed slower water release rate when compared with that of other reported polymer microcapsules (e.g. water release slopes of carboxylic acid, sulfonic acid and imidazole polymer microcapsules being 0.04, 0.055 and 0.053, respectively) [5]. Such results further indicated that tuning hydrophilicity–hydrophobicity of PMCs provided an effective approach to slow down the water release rate of PMCs. For PMC-IV, the abnormal high water release rate may be owing to the rather low content of bound water.

Fig. 7 showed the water release of all the membranes, at 40 °C and 20% RH, following similar processes: rapid evaporation of free water in the first step (0–30 min); slow water evaporation of bound water in the second step (from 30 to 180 min). The SPEEK control membrane suffered from serious water loss especially at the first step, and 99.7% of the absorbed water evaporated after 180 min testing. Encouragingly, the embedment of PMC reduced water loss to the range of 88.5–66.1% for the membranes based on PMC-III (Fig. 7c). For the composite membranes, the water release rate decreased in the order of SPEEK/PMC-IV > SPEEK/PMC-I > SPEEK/PMC-II > SPEEK/PMC-III, in accordance with that of the PMCs.

3.3.3. Water retention

Due to the high water uptake and slow water release, PMC-III displayed the highest water retention, whereas PMC-IV displayed the lowest water retention, as shown in Fig. 6b. The incorporation of the PMCs remarkably improved the water retention of the composite membranes, and water retention increased from 0.1% for the SPEEK control membrane up to 19.4% for 15 wt% PMC-III filled membrane after 180 min testing, which can be seen in Fig. 8. The water retention of the composite membranes decreased in the order of SPEEK/PMC-III > SPEEK/PMC-II > SPEEK/PMC-I > SPEEK/PMC-IV. All these data revealed that manipulating hydrophilicity–hydrophobicity of PMCs provided an effective approach to enhance their water retention properties.

3.4. Proton conductivity of the membranes

Proton conductivity of the proton exchange membrane is a key parameter determining fuel cell performance. The proton conductivity at 25 °C and 100% RH of the membranes was presented in Table 2, which revealed that the embedment of PMCs obviously facilitated proton conduction. The SPEEK control membrane displayed a proton conductivity of 0.0138 S cm^{-1} and 15 wt% fillers derived membranes showed enhanced proton conductivity up to 0.0176, 0.018, 0.0182 and 0.0165 S cm^{-1} for SPEEK/PMC-I, SPEEK/PMC-II, SPEEK/PMC-III, and SPEEK/PMC-IV, respectively. The PMC-III filled membranes displayed a more pronounced enhancement of proton conductivity compared with that of composite membranes based on other PMCs. It was known that –COOH groups possessed a lower degree of dissociation compared to that of the $-SO_3H$ groups, and hence –COOH polymer filler will decrease the ion-exchange capacity of SPEEK membrane, which in turn will decrease the Grotthuss-type transfer. Therefore, the enhancement of proton conductivity may be arisen from that the enhanced water uptake facilitated the protonation of water to form hydronium ion and enhanced proton mobility, thus intensifying the proton transport.

To understand the relations between water retention and proton conductivity, time-dependent conductivity of the membranes under 20% RH was tested, as shown in Fig. 9. Proton conductivity displayed a tendency of decline over time for all the membranes, indicating the dependence of proton transport on water content. The proton conductivity of the SPEEK control membrane displayed a reduction of 93% from 1.36×10^{-2} S cm^{-1} to 9.54×10^{-4} S cm^{-1} within 90 min testing. The reduction should be ascribed to the substantial dehydration giving rise to shrinkage and disconnection of the proton conduction nanochannels. Encouragingly, the embedment of PMCs considerably retarded the proton conductivity decline of the composite membranes due to the suppression of dehydration. For instance, the conductivity reduction is 33.9% (from 1.90×10^{-2} to 6.95×10^{-3} S cm^{-1}), 32.1% (from 2.79×10^{-2} to 7.12×10^{-3} S cm^{-1}), 26.0% (from 3.42×10^{-2} to 1.17×10^{-2} S cm^{-1}), and 38.9% (from 1.52×10^{-2} to 9.27×10^{-3} S cm^{-1}) during the measurement when incorporating 15 wt% PMC-I, PMN-II, PMC-III and PMC-IV, respectively. The loss of proton conductivity of the membranes has a positive correlation with the loss of water,

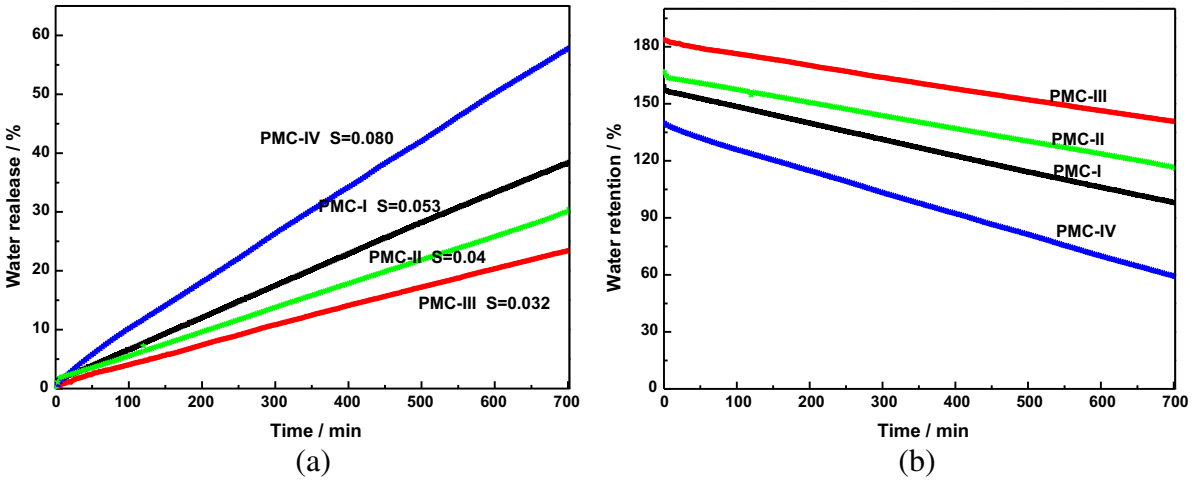

Fig. 6. (a) Water release, (b) water retention of the PMCs as a function of time at 40 °C and 20% RH.

consistent with the previous studies [5,6]. The PMC-III exhibited more pronounced effect in retarding the decline of proton conductivity compared with the previous studies. The main reason was that the PMCs in this work possessed better water retention properties, which was helpful for vehicle-type proton conduction. The membrane with better water retention showed more stable proton conductivity under low RH, implying that water content in PEM strongly influenced the proton migration. The stability of proton conductivity revealed that the microcapsules, serving as water reservoirs like the vacuoles in plant cell [38], could release

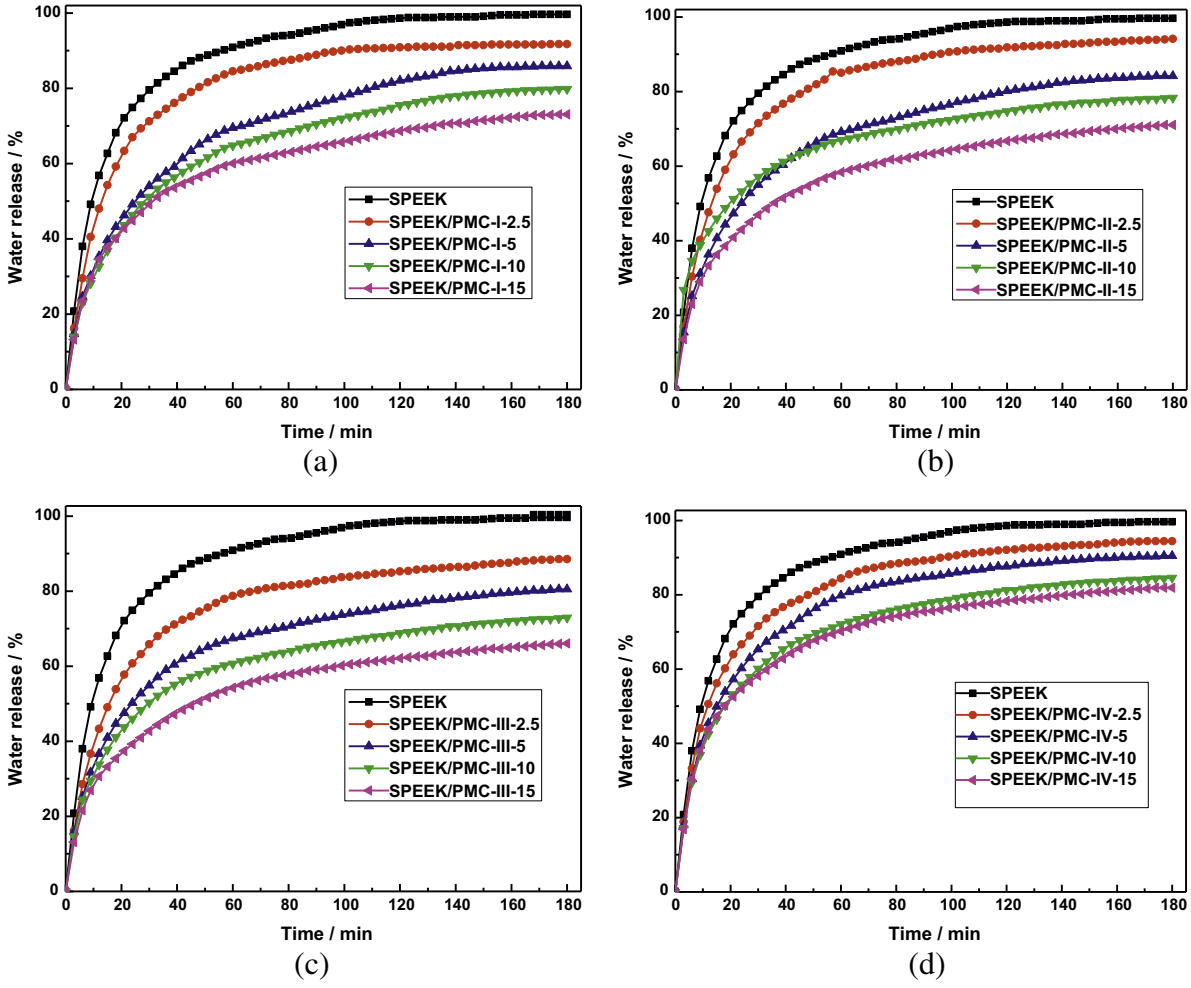

Fig. 7. Water release of the membranes as a function of time at 40 °C and 20% RH.

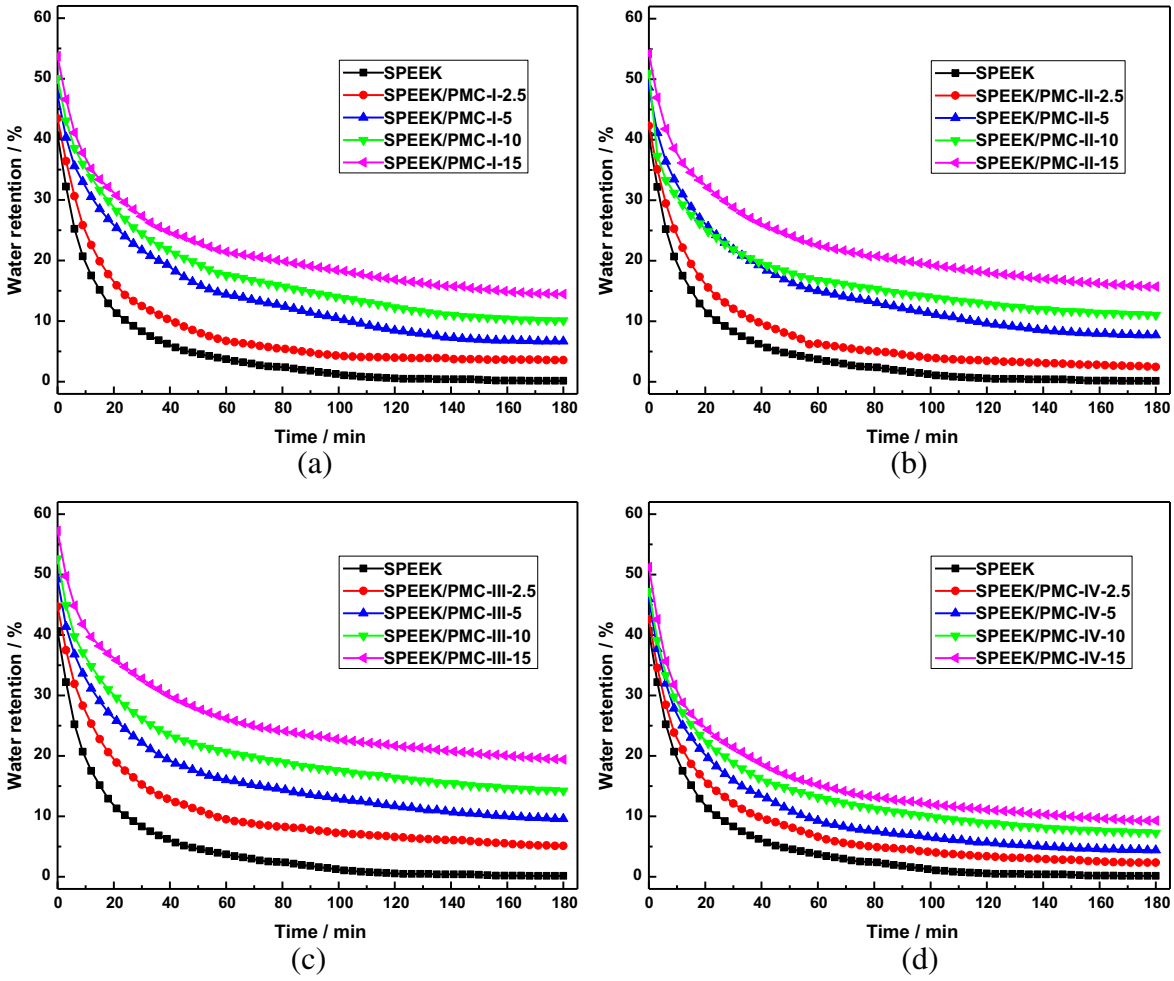

Fig. 8. Water retention of the membranes as a function of time at 40 °C and 20% RH.

water into SPEEK bulk in a controllable way to retard the dehydration of the membrane and retain its proton conduction. Since PMCs could confer good water retention property to the corresponding composite membrane, it could be conjectured that higher low-humidity proton conductivity can be obtained if Nafion were employed as the matrix polymer [4], in comparison with the case of SPEEK.

The Arrhenius plot of conductivity for the SPEEK/PMC-III membranes and the SPEEK control membrane in the temperature range of 30–75 °C was depicted in Fig. 9. All the membranes exhibited positive temperature-conductivity correlations, which implied a thermally activated process. Activation energy of proton conductivity (E_a) for the membranes was calculated according to the Arrhenius equation and displayed in Fig. 10. The gradual decline of the activation energy with increasing PMC-III content in SPEEK matrix suggested the decreased energy barrier for proton transfer [39]. A plausible explanation was that the PMCs provided additional pathway at the water-rich SPEEK/PMC interface for rapid proton transfer.

3.5. Methanol crossover of the membranes

High methanol barrier property (methanol permeability $< 10^{-6}$ cm^2 s^{-1}) is essentially desired for the PEM used in direct methanol fuel cells (DMFCs) to diminish the mixed potential effect and catalyst poisoning [40]. The methanol permeability of the membranes at room temperature was evaluated and the results were summarized in Table 2. The data revealed that the incorporation of PMCs notably reduced the methanol crossover of the SPEEK membranes. Methanol permeability reduced from 9.1×10^{-7} cm^2 s^{-1} for SPEEK control membrane to 6.3×10^{-7} cm^2 s^{-1} for the membrane based on 15 wt% loading of PMC-IV, with a 30.8% reduction. Increasing the filler content endowed the composite membranes with gradually intensified methanol barrier properties. The improved methanol barrier properties should be ascribed to the presence of PMCs with a highly cross-linked structure which resulted in a tortuous and prolonged methanol diffusion pathway [11]. Another interesting finding in Table 2 was that the methanol barrier properties improved in the order of SPEEK/PMC-I < SPEEK/PMC-II < SPEEK/PMC-III < SPEEK/PMC-IV, in line with the increasing order of membrane hydrophobicity. This behavior may be arisen from that the relatively hydrophobic PMCs render the composite membranes more hydrophobic, which could prevent methanol from being absorbed into the composite membranes [41].

4. Conclusion

In this study, four kinds of carboxylic acid polymer microcapsules with different hydrophilicity–hydrophobicity were synthesized and incorporated into the SPEEK matrix to prepare composite membranes. Manipulating the hydrophilicity–hydrophobicity of

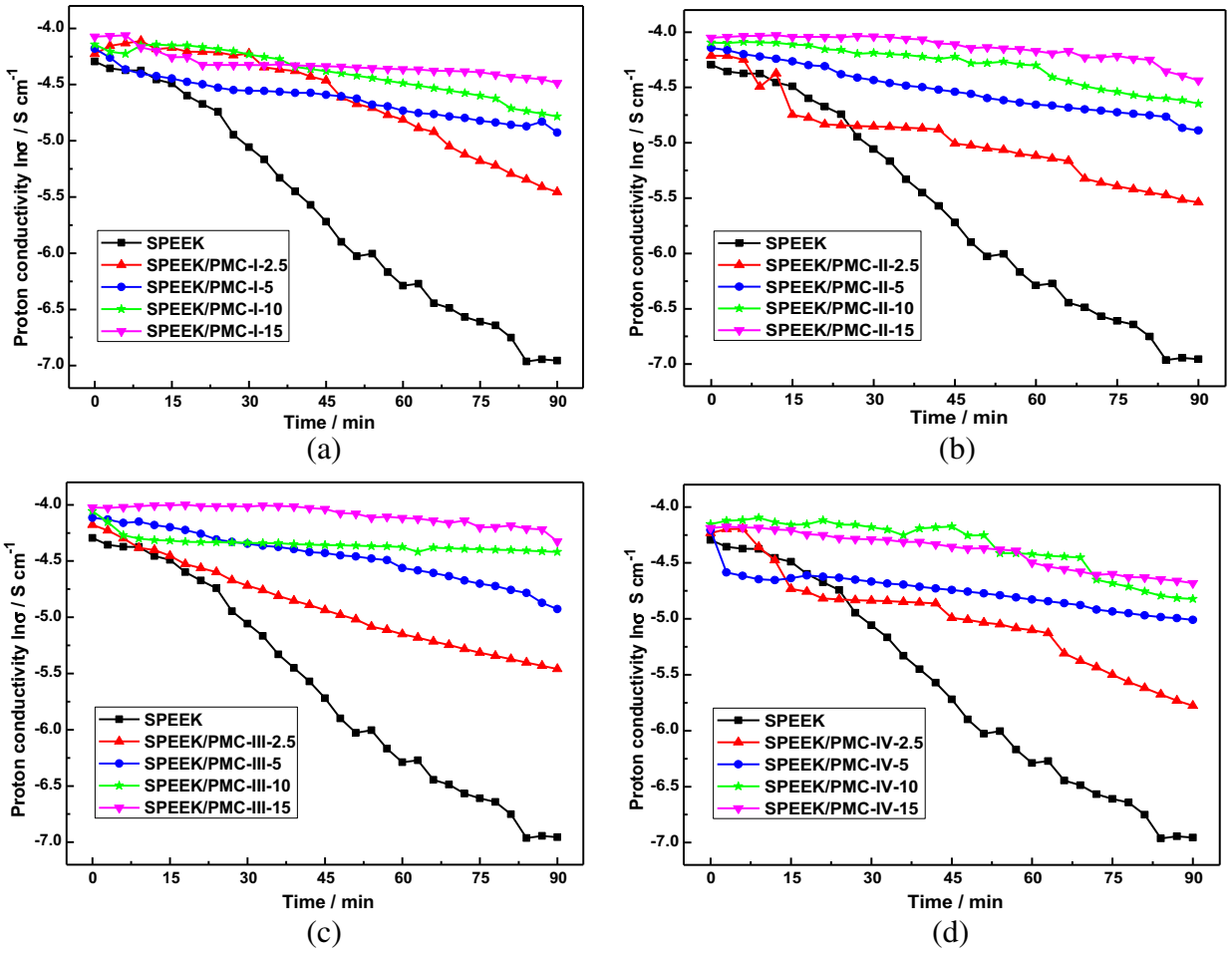

Fig. 9. Time-dependent proton conductivity of the membranes at 40 °C and 20% RH.

polymer microcapsules was demonstrated as an effective approach to improve their water retention properties. The PMCs with appropriate hydrophilic/hydrophobic balance endowed the membranes with unusual water retention properties, and hence superior proton conductivity under low RH. The membrane with 15 wt% PMC-III displayed the highest proton conductivity of 0.0132 S cm^{-1} at 40 °C and 20% RH after 90 min testing, about thirteen times higher than that of the SPEEK control membrane. Moreover, the PMCs can reduce the activation energy for proton conduction of the SPEEK membranes and the methanol permeability through the membranes. Considering the controllable water retention and desirable proton conduction properties of the PMCs, the present study may contribute to rational design of water retention materials, and the PMCs may find application in diverse energy fields.

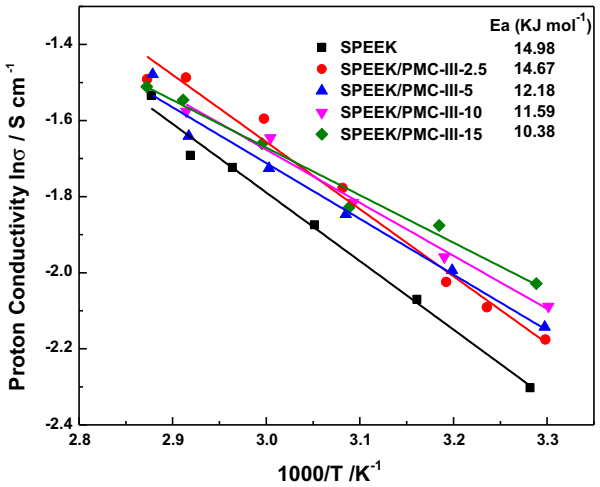

Fig. 10. Temperature-dependent proton conductivity of the SPEEK/PMC-III membranes and the SPEEK control membrane at 100% RH.

Acknowledgments

We gratefully acknowledge financial support from National Science Fund for Distinguished Young Scholars (21125627), the National High Technology Research and Development Program of China (2012AA03A611), and the Program of Introducing Talents of Discipline to Universities (No. B06006). Thanks Dr. Jingtao Wang, Zhengzhou University, China for their valuable help in this study.

References

[1] A.P.R. Johnston, C. Cortez, A.S. Angelatos, F. Caruso, Curr. Opin. Colloid Interface Sci. 11 (2006) 203–209.
[2] W. Tong, X. Song, C. Gao, Chem. Soc. Rev. 41 (2012) 6103–6124.
[3] X. Liu, A. Basu, J. Am. Chem. Soc. 131 (2009) 5718–5719.
[4] H. Pu, D. Wang, Z. Yang, J. Membr. Sci. 360 (2010) 123–129.
[5] J. Wang, H. Zhang, X. Yang, S. Jiang, W. Lv, Z. Jiang, S.Z. Qiao, Adv. Funct. Mater. 21 (2011) 971–978.

[6] J. Wang, X. Yue, Z. Zhang, Z. Yang, Y. Li, H. Zhang, X. Yang, H. Wu, Z. Jiang, Adv. Funct. Mater. 22 (2012) 4539–4546.
[7] A. Chandan, M. Hattenberger, A. El-kharouf, S. Du, A. Dhir, V. Self, B.G. Pollet, A. Ingram, W. Bujalski, J. Power Sources 231 (2013) 264–278.
[8] C.H. Park, C.H. Lee, M.D. Guiver, Y.M. Lee, Prog. Polym. Sci. 36 (2011) 1443–1498.
[9] V. Ramani, H.R. Kunz, J.M. Fenton, J. Power Sources 152 (2005) 182–188.
[10] J. Yang, P.K. Shen, J. Varcoe, Z. Wei, J. Power Sources 189 (2009) 1016–1019.
[11] J. Wang, Z. Zhang, X. Yue, L. Nie, G. He, H. Wu, Z. Jiang, J. Mater. Chem. A 1 (2013) 2267.
[12] L. Lou, H. Pu, Int. J. Hydrogen Energy 36 (2011) 3123–3130.
[13] L. Nie, H. Dong, X. Han, G. He, H. Wu, Z. Jiang, J. Power Sources 240 (2013) 258–266.
[14] B. Guo, S.W. Tay, Z. Liu, L. Hong, Polymers 4 (2012) 1499–1516.
[15] Y. Li, H. Jia, Q. Cheng, F. Pan, Z. Jiang, J. Membr. Sci. 375 (2011) 304–312.
[16] G. Kerstiens, J. Exp. Bot. 57 (2006) 2493–2499.
[17] L. Kunst, A.L. Samuels, Prog. Lipid Res. 42 (2003) 51–80.
[18] G. Vogg, S. Fischer, J. Leide, E. Emmanuel, R. Jetter, A.A. Levy, M. Riederer, J. Exp. Bot. 55 (2004) 1401–1410.
[19] F.S. Majedi, M.M. Hasani-Sadrabadi, S.H. Emami, M. Taghipoor, E. Dashtimoghadam, A. Bertsch, H. Moaddel, P. Renaud, Chem. Commun. 48 (2012) 7744–7746.
[20] G.L. Li, H. Mohwald, D.G. Shchukin, Chem. Soc. Rev. 42 (2013) 3628–3646.
[21] G. Gebel, Macromolecules 46 (2013) 6057–6066.
[22] X. Wu, G. He, X. Li, F. Nie, X. Yan, L. Yu, J. Benziger, J. Power Sources 246 (2014) 482–490.
[23] W. Stöber, A. Fink, J. Exp. Bot. 26 (1968) 62–69.
[24] G. Wei, L. Xu, C. Huang, Y. Wang, Int. J. Hydrogen Energy 35 (2010) 7778–7783.
[25] F. Bai, X. Yang, R. Li, B. Huang, W. Huang, Polymer 47 (2006) 5775–5784.
[26] J. Wang, S. Jiang, H. Zhang, W. Lv, X. Yang, Z. Jiang, J. Membr. Sci. 364 (2010) 253–262.
[27] G. Li, X. Yang, F. Bai, Polymer 48 (2007) 3074–3081.
[28] Y. Li, J. Ma, React. Funct. Polym. 50 (2001) 57–65.
[29] Y. Zhang, S. Wei, F. Liu, Y. Du, S. Liu, Y. Ji, T. Yokoi, T. Tatsumi, F.-S. Xiao, Nano Today 4 (2009) 135–142.
[30] M. Roice, K.S. Kumar, V.N.R. Pillai, Macromolecules 32 (1999) 8807–8815.
[31] T. Yang, L. Meng, N. Huang, J. Power Sources 224 (2013) 132–138.
[32] Y. Zhao, Z. Jiang, L. Xiao, T. Xu, H. Wu, J. Power Sources 196 (2011) 6015–6021.
[33] P. Xing, G.P. Robertson, M.D. Guiver, S.D. Mikhailenko, K. Wang, S. Kaliaguine, J. Membr. Sci. 229 (2004) 95–106.
[34] Y. Zhao, Z. Jiang, D. Lin, A. Dong, Z. Li, H. Wu, J. Power Sources 224 (2013) 28–36.
[35] K.D. Kreuer, Chem. Mater. 8 (1996) 610–641.
[36] M.K. Mistry, N.R. Choudhury, N.K. Dutta, R. Knott, Z. Shi, S. Holdcroft, Chem. Mater. 20 (2008) 6857–6870.
[37] H.M.L. Thijs, C.R. Becer, C. Guerrero-Sanchez, D. Fournier, R. Hoogenboom, U.S. Schubert, J. Mater. Chem. 17 (2007) 4864.
[38] C. Stock, H.K. Grønlien, R.D. Allen, Y. Naitoh, J. Cell Sci. 115 (2002) 2339–2348.
[39] Z. Jiang, X. Zhao, Y. Fu, A. Manthiram, J. Mater. Chem. 22 (2012) 24862.
[40] H. Ahmad, S.K. Kamarudin, U.A. Hasran, W.R.W. Daud, Int. J. Hydrogen Energy 35 (2010) 2160–2175.
[41] S.Y. So, S.C. Kim, S.-Y. Lee, Solid State Ionics 181 (2010) 714–718.